Diesel engine optimisation, with emissions constraints, on a prescribed driving route

Conference Proceedings (Accepted Version)

Pease, Gareth, Limebeer, David and Fussey, Peter (2017) Diesel engine optimisation, with emissions constraints, on a prescribed driving route. IEEE AFRICON 2017, Cape Town, 18-20 September 2017. Published in: Cornish, Darryn R, (ed.) 2017 IEEE AFRICON. Institute of Electrical and Electronics Engineers ISSN 2153-0033 ISBN 9781538627754

Diesel Engine Optimisation, with Emissions Constraints, on a Prescribed Driving Route

Gareth Pease
Department of
Engineering Science
University of Oxford
Oxford, UK, OX1 3PJ
Email: gareth.pease@eng.ox.ac.uk

David Limebeer
Department of
Engineering Science
University of Oxford
Oxford, UK OX1 3PJ
Email: david.limebeer@eng.ox.ac.uk

Peter Fussey
Ricardo UK Plc
Shoreham-by-Sea,
West Sussex, UK, BN43 5FG
Email: peter.fussey@ricardo.com

***Abstract*—A method for evaluating driving technique and engine operation, with emissions constraints, on a real driving route, is presented. A single degree of freedom vehicle model with simple resistive forces is driven along the pre-planned route. Instead of the velocity trajectory being determined *a priori*, the optimisation can choose the optimal speed along the route as well as the engine operating point. When constraints on the total emissions are imposed, the engine no longer operates on the minimum fuel locus; the power delivery changes as the emissions constraints are tightened. The driving technique changes from a series of bang-bang switches, into a smoother application of the engine power. The route is driven in the absence of stops and traffic restrictions.**

***Keywords*—Trajectory optimisation, nonlinear programming, automotive engineering, vehicle propulsion**

I. Introduction

In recent years it has become increasingly apparent that there are a number of shortcomings in vehicle emissions testing. With the road car industry under scrutiny, there is increased social and political pressure to ensure emissions testing methods represent the real world driving of vehicles. There are two ways to improve the fuel economy for a road vehicle: driving more economically (by avoiding unnecessary acceleration and braking) and using the engine more economically (operating at a more efficient operating point). Therefore, it is beneficial to be able to model and optimise the entire route for both driving style and engine operation.

Historically, to appraise engine design and ensure that engine operation conforms to emissions limits, standardised test cycles are used. These take the form of a pre-planned velocity profile designed to represent driving conditions in most scenarios. One of the most widely used is the New European Drive Cycle (NEDC). A significant drawback is that predefined cycles, with their prescribed velocity profiles, do not accommodate changes in driving technique.

Analytical results based on Pontryagin's Maximum Principle were presented for an eco-driving optimal control problem in [1]. The optimal driving for each segment can be split into a number of distinct phases: maximum power acceleration, constant speed, coasting, followed by maximum power braking. The switching times for each of these segments form the basis for a dynamic programming algorithm. As the

Fig. 1. Exemplar 28km driving route.

optimisation is limited to only 200 metres, the assumption that the road is of constant slope is a reasonable one. A method for controlling a diesel engine, with comparison to a parallel hybrid, was the basis of the work in [2]. Optimisation of the power delivery in combination with the aftertreatment devices is considered. The fuel optimal control strategy has to incorporate the energy/emissions storage ability of the powertrain as well. The results of the optimisation show that it is no longer simply a matter of choosing the engine operating point based on the fuel efficient curve.

Utilising route information is an important recent development, which is made possible by sophisticated GPS devices that are the norm in most new production vehicles. Adaptive cruise control is in lorries is one possible application [3]. Fuel and journey time savings were made possible when the cruise controller was able to 'preview' the road gradient.

The use of optimal control to optimise both the driving style and the powertrain power split for a vehicle equipped with a hybrid powertrain was the subject of [4]. A short route is considered through the countryside in order to ignore the effects of traffic. The methods used highlight the benefits to optimising both the power usage and the driving profile. This has the benefit of removing the requirement for a prescribed velocity profile normally required for power split optimisation. A number of different optimisation techniques were used in [5] to great effect. Typical driving can be split into a number of sub-problems each with their own solution structure. The results of the optimal control form the basis of an eco-driving guideline depending on the scenario under consideration.

A pseudospectral method was employed to solve the optimal fuel economy optimal power split problem for a series hybrid electric bus in [6]. This was shown to be computationally more efficient than a standard dynamic programming approach.

In general, the power and velocity optimisation for hybrid vehicles requires the use of the fuel-optimal engine operating trajectory [7]. While this remains the optimal brake-specific engine operation in terms of fuel consumption, it is unclear how this will change under emissions constraints. For a fixed-power trajectory (and its velocity trajectory), the optimisation is more straight-forward. However, it is not necessarily optimal to drive in the same manner in terms of fuel consumption. It may result in the route being traversed more rapidly for some constraints in order to minimise the fuel consumption. This is the way in which drive cycles are used to evaluate and optimise engine performance.

The majority of engine-based optimisation techniques discussed so far require the use of dynamic programming (DP) or a pseudo-DP algorithm. The 'curse of dimensionality' occurs when the problem becomes increasingly complex due to the increased number of decision variables. Additionally, the problem is solved for a fixed time step across the whole horizon. In the case that there are features that are highly non-linear, it is advantageous to allow the solution mesh to be varied [8]. This method works well within a direct method for solving the optimal control problem.

This document presents some preliminary work for modelling and optimisation of a vehicle along a real world driving route (Fig. 1) in the absence of traffic and enforced stoppages. The problem is split into a number of phases wherein the velocity limit within each is given by the legislative limit in that segment. The results of the optimisation are designed for a pre-trip insight into the most economical vehicle velocity and power usage. The problem is solved with a direct collocation method to ensure that the total emissions constraints are met for the duration of the journey.

II. Fuel Minimisation Optimal Control Problem

A. Vehicle Model

The dynamics governing the vehicles progression along the route can be formed using a force balance parallel to the slope and Newton's Second Law (Fig. 2).

$$\dot{v}(t) = \frac{1}{M}\Big(F_t(t) - F_r(t) - Mg\sin\theta(t)\Big) \tag{1}$$

where M is the vehicle mass, g is the acceleration due to gravity. The control input is the tractive power $P_t(t)$ available at the wheels. The tractive power is related to the tractive force by

$$F_t(t) = \frac{P_t(t)}{v(t)} \tag{2}$$

where it is assumed that the power delivery is instantaneous, with no dynamics between the engine delivered power and the required tractive power. The resistive force F_r is made

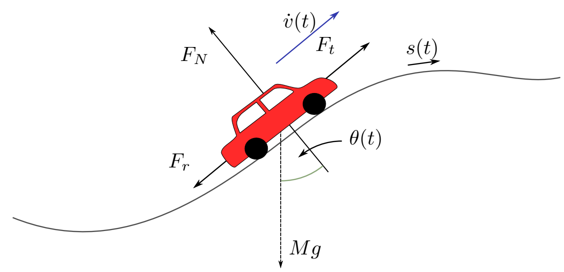

Fig. 2. The force system acting on the car.

up of two components - the aerodynamic drag and the rolling resistance.

$$F_r(t) = \frac{1}{2}\rho C_d A v(t)^2 + \mu F_N(t) \tag{3}$$

where C_d is the coefficient of aerodynamic drag, A is the vehicle frontal area, ρ the density of air and μ the rolling resistance coefficient. The normal reaction is the perpendicular component of the weight $F_N(t) = Mg\cos\theta(t)$.

B. Powertrain Model

The engine used in this study is a small 1.7l diesel engine with data taken from the free ADVISOR software package [9]. The engine is linked to the wheels via a continuously variable transmission (CVT). The CVT removes the need to constrain the engine rotational speed relative to the wheel rotational speed. The engine power is given by $P_e(t) = \omega_e(t)\tau_e(t)$, where $\omega_e(t)$ and $\tau_e(t)$ are the engine angular velocity and torque respectively. The fuel flow is given by the engine map (taken from [9])

$$\dot{m}_f = g(\omega_e, \tau_e). \tag{4}$$

which is represented in the optimal control calculation by the bi-quadratic map

$$g(\omega_e,\tau_e) = 0.2903 + 0.0021298\omega_e + 0.00198\tau_e \\ +2.2745\times10^{-6}\omega_e^2 - 2.2619\times10^{-6}\tau_e^2 + 4.58924\times10^{-5}\tau_e\omega_e. \tag{5}$$

Similarly to the fuel map, NO_x and PM maps are available in the ADVISOR software package. These form the emissions models for the integral constraints imposed on the problem.

C. Optimal Control Problem

The fuel-optimal control problem can now be posed. It is necessary to transform the problem from the time domain, t, to the distance travelled domain, s, to ensure that the route information can be properly utilised in the problem. This is a reasonable transformation as both quantities will be

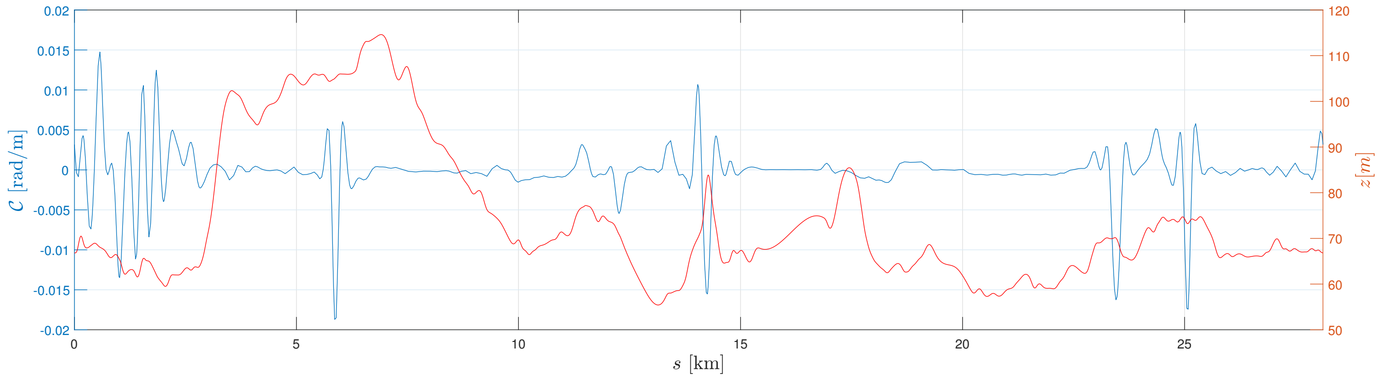

Fig. 3. The optimal curvature (plotted in blue) and elevation (plotted in red) estimate around the route.

monotonically increasing along the test route (as $v(t) > 0$). Changing the independent variable is achieved using

$$ds = v(s)dt. \tag{6}$$

The cost function is the total fuel usage along the route, and is given by the following integral

$$m_{fuel} = \int_0^{s_f} g(\omega_e(s), \tau_e(s)) \frac{\mathrm{d}s}{v(s)}, \tag{7}$$

where $g(\omega_e(s), \tau_e(s))$ is given by (5). The system dynamics can be written concisely as

$$\frac{dv(s)}{ds} = f(v(s), \mathbf{u}(s)) \tag{8}$$

where the control vector is

$$\mathbf{u}(s) = \begin{bmatrix} P_t(s) \\ \omega_e(s) \\ \tau_e(s) \end{bmatrix}. \tag{9}$$

and the corresponding state equation is given by the right hand side of Eqn. (1). The lateral acceleration is constrained by

$$|\mathcal{C}(s)|v(s)^2 \leq \zeta, \tag{10}$$

in which $\mathcal{C}(s)$ is the geodesic curvature. Additionally, the forward velocity is also constrained by

$$v(s) \leq v_l(s), \tag{11}$$

which represents legislative speed limits. In addition to the drive-ability limit governed by the lateral acceleration limit, it is also necessary to introduce a longitudinal acceleration limit

$$\underline{a}_l \leq f(v(s), \mathbf{u}(s)) \leq \overline{a}_l. \tag{12}$$

which, in combination with (10), represents a simple rectangular g g diagram for the vehicle. Power balance between the powertrain and the car is modelled with the following inequality

$$P_e(s) - P_t(s) \geq 0. \tag{13}$$

The tractive power is bounded by the maximum engine power $P_{e,max}$ and the maximum braking power P_b. The engine operating points are limited to remain on the maps in Fig. 4:

$$\underline{\tau_e} \leq \tau_e \leq \overline{\tau_e}(\omega_e) \tag{14}$$

$$\underline{\omega_e} \leq \omega_e \leq \overline{\omega_e} \tag{15}$$

The upper limit on the engine torque is governed by the maximum torque line - plotted in red in Fig. 4. The boundary conditions on the state are

$$v(0) = v(s_f) = \epsilon, \tag{16}$$

where ϵ is a small positive number to ensure the vehicle starts and ends close to rest, but does not cause the problem to run into numerical issue. Finally it is necessary to impose a number of integral constraints. The first of which is the upper bound on the arrival time

$$T = \int_{s_0}^{s_f} \frac{1}{v(s)} ds \leq T_{max}. \tag{17}$$

The bound on T acts as a surrogate for the driving style, a lower arrival constraint implies more aggressive driving style. There are also limits on the total amount of emissions which can be produced

$$\int_0^{s_f} \dot{m}_{\mathrm{NO_x}}(\omega_e(s), \tau_e(s))ds \leq \overline{m}_{\mathrm{NO_x}} \tag{18}$$

$$\int_0^{s_f} \dot{m}_{\mathrm{PM}}(\omega_e(s), \tau_e(s))ds \leq \overline{m}_{\mathrm{PM}}. \tag{19}$$

D. Route Model

Route information is obtained as raw GPS data which is transformed into a local x-y-z co-ordinate frame. In order to gain a smooth set of data for both the track slope and the curvature, an optimal filtering problem can be posed. This smoothing will aid in the solution of the fuel optimisation. For brevity only the elevation estimation problem is presented here, the curvature estimate is calculated in the same manner as the centre of a racing track in [10].

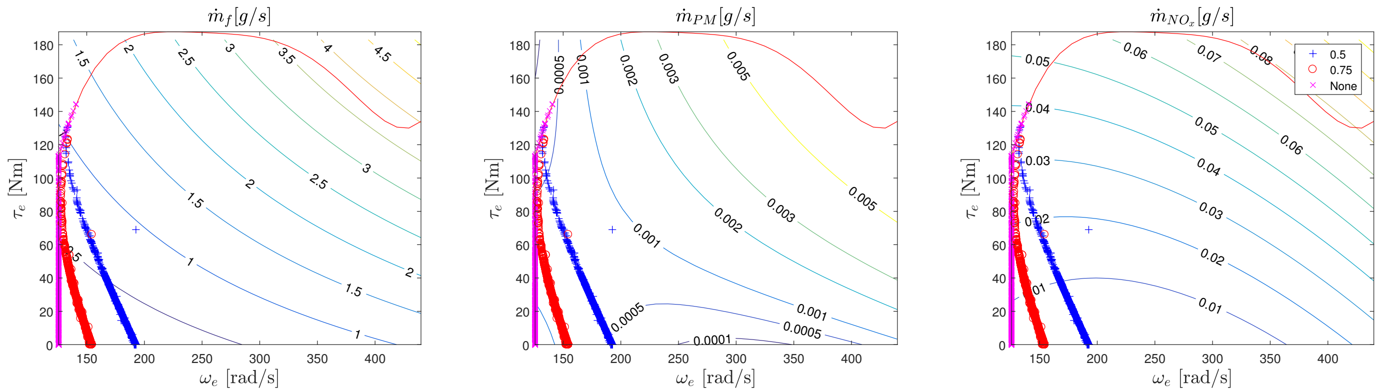

Fig. 4. Scatter of engine operating points for the three runs: unconstrained (magenta cross), three-quarters of the production of NO_x and PM (red circles), and half of the production of NO_x and PM (blue plus).

The dynamics of the filtering problem for the slope estimation can be posed as such[1]:

$$\begin{aligned} \dot{z}(s) &= \theta(s) \\ \dot{\theta}(s) &= u(s). \end{aligned} \tag{20}$$

The dot notation represents the derivative with respect to displacement. It is necessary to have both the elevation, $z(s)$, and the gradient of the track, $\theta(s)$, as states to enforce continuity at the beginning and end of the loop.

$$\begin{aligned} z(0) &= z(s_f) \\ \theta(0) &= \theta(s_f). \end{aligned} \tag{21}$$

A performance index which incorporates both the magnitude of the error between the GPS data and a regularisation term can be formed

$$J = \int_0^{s_f} (z(s) - z_{GPS}(s))^2 + \omega u(s)^2 ds. \tag{22}$$

The weighting factor ω (in this case 10^5) allows for a varied amount of smoothing between the estimate of the gradient and the estimate of the elevation of the track. Fig. 3 shows the results of both the curvature and elevation estimation problems as a function of the route length.

E. Numerical Optimal Control

The optimal control problem is solved with an adaptive Legendre-Gauss-Radau direct collocation method which is implemented in GPOPS-II [11]. Derivative information is provided by automatic differentiation software (ADiGator [12]) and the arising non-linear program is solved with the interior point method using IPOPT [13].

III. Results

Several variants of the problem were solved in order to gain insight into the powertrain usage over the route. The problem data is available in Table I. It is expected that the fuel-minimum optimum will require the vehicle minimal fuel usage while avoiding unnecessary braking. A preliminary study for an arrival time of 2100 seconds is considered to investigate the minimum fuel solution structure. For the most part the optimal tractive power operation takes the form of bang switches (see Fig. 5) between 0 torque and the intersection of the maximum torque line. It is well known that unnecessary braking is detrimental to the fuel consumption as the vehicle has to be re-accelerated to return to the previous speed. Considering the second plot in Fig. 5 one can see that the power application occurs whenever the car is required to ascend hills. Fuel is subsequently saved on the descents.

For the same arrival time of 2100 seconds, a comparison of the power strategy when emissions constraints are introduced is investigated. The optimal engine operation is no longer on the locus corresponding to the minimum fuel consumption. The red and blue scatters in Figure 4 show the deviation for a reduction of three-quarters of the total emissions and half the total emissions. The effect of this on the power usage is quite stark. It is no longer optimal to run the engine in a bang-bang fashion, but rather to maintain a much more smooth power delivery (Fig. 7). This is due to the new operating line no longer coinciding with the torque axis of the fuel map. The power usage is the same for each of the segments when the velocity constraint is active however. Due to the increased

TABLE I
TABLE OF THE VEHICLE PARAMETERS USED IN THE NUMERICAL OPTIMISATION.

Symbol	Value
M	$1280kg$
A	$2m^2$
C_d	0.3
ρ	$1.2kg/m^3$
ζ	$0.1g\ m/s^2$
μ	0.01
$\underline{a}_l$	$-0.1g\ m/s^2$
$\overline{a}_l$	$+0.1g\ m/s^2$
ϵ	$0.01m/s$

[1]It should be noted that $\theta(s)$ should really be defined as $\theta(s) = \tan^{-1}(\frac{dz}{ds})$. A small angle approximation can be used to simplify the optimal control problem, i.e $\theta(s) \approx \frac{dz}{ds}$ as the expected gradients are small.

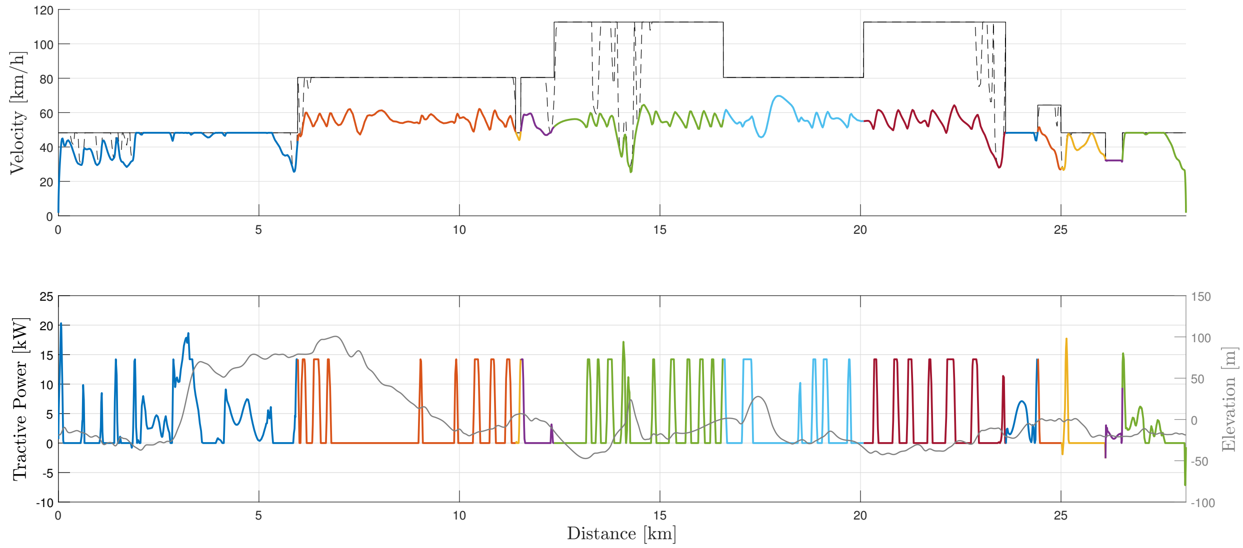

Fig. 5. Evolution of the velocity state for an arrival time of 2100 seconds. The legislated speed limit is plotted in black and the lateral acceleration limit is plotted as a dashed line. The second plot shows the tractive power P_t along with the route elevation. Each of the phases of the optimal control problem is plotted separately for clarity.

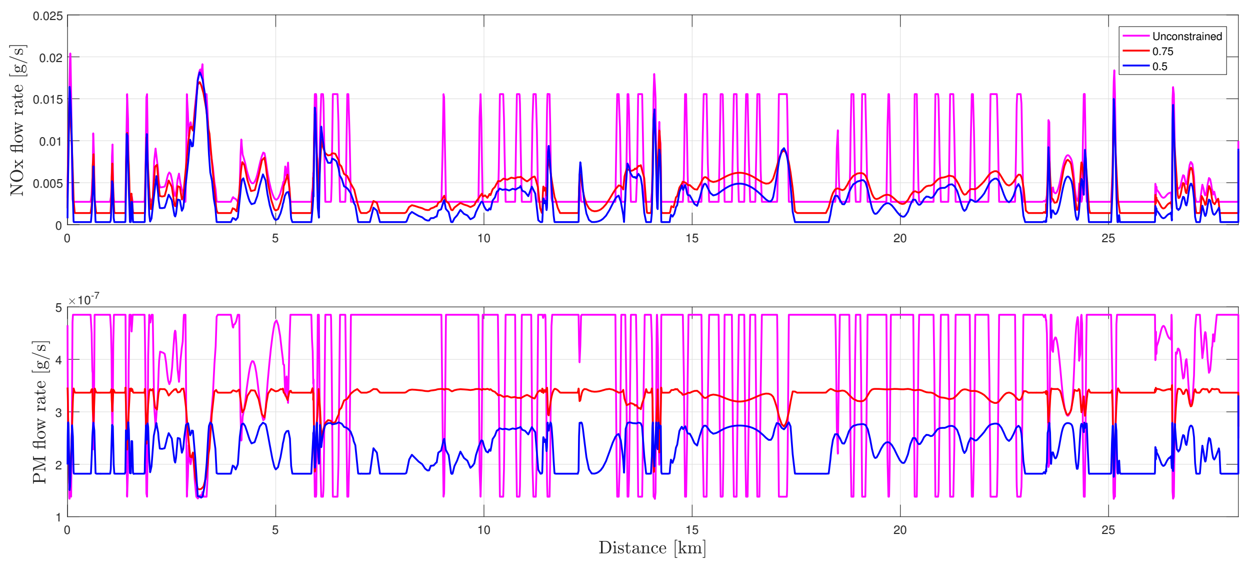

Fig. 6. The flow rates of NO_x (top) and PM (bottom). Unconstrained is plotted in magenta, while the constrained runs are in red (0.75) and blue (0.5).

power usage, the arrival time is now shorter for the emissions constrained, 2008 seconds and 1964 seconds compared to the full arrival time for the unconstrained run.

TABLE II
A COMPARISON OF THE NUMERICAL VALUES AND COMPUTATION TIME.

Limit	$m_{\mathrm{NO_x}}$ (g)	m_{PM} (g)	m_f (g)	T (s)	Comp. Time (s)
0.5	10.346	1.111	678.93	1964.7	94.312
0.75	15.519	1.6665	487.15	2008.7	151.95
None	20.692	2.2219	364.71	2100	217.59

IV. CONCLUSIONS AND FURTHER WORK

A simple vehicle model, suitable for optimal control studies, is used to describe the motion of a car along a prescribed route. The travelled route is modelled as a 3D curve, which is estimated from measured GPS data, has elevation changes as well as corners. A lateral acceleration limit is imposed that is a function of the path curvature. Legislated speed limits are incorporated into the problem as a sequence of speed constraints by splitting the problem into a number of phases. Fuel and emissions maps are appended to the vehicle model to represent the engine operation during driving. Artificial limits on emissions production can be used to gain insight into different modes of engine operation. The presented results show the effectiveness of the direct collocation method for solving this particular optimal control problem, with solution times typically under five minutes on a standard desk top

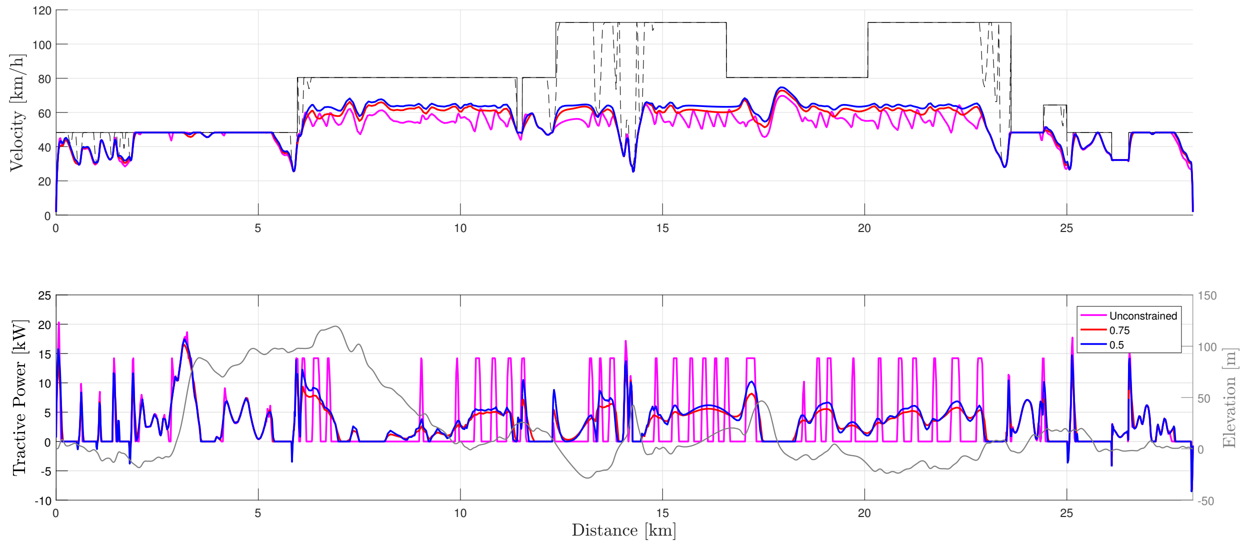

Fig. 7. Optimal velocity and power trajectory comparison for an arrival time of 2100 seconds. The legislative speed limit is plotted in black with the curvature limit as the black dashed line. The elevation of the route is plotted in grey.

computer. As a result, there is flexibility available to make the problem more complex without unreasonably long solution times.

Exhaust Gas Recirculation (EGR) has become an industry standard for reducing emissions by diluting the intake manifold air; this has an negative impact on the fuel consumption. It is necessary to include a higher-dimensional model for NO_x which could take the form of a stochastic spatial model to include further control inputs (for example boost pressure in the case that the engine is turbocharged). This has a detrimental effect on fuel economy, which may be offset via the usage of a hybrid powertrain. This extension would be reasonably simple to implement within the direct collocation optimisation framework. It is assumed in this work that the car does not stop at traffic lights, nor is hindered by other traffic. By changing the velocity constraints, these could be added in as future work. The results presented offer insight into optimal power deployment along the route. This could form the basis of a pre-trip driving advisor, which offers the most fuel efficient way for the driver to use the vehicle.

Acknowledgements

This work was part funded by the Engineering and Physical Life Sciences Research Council and Ricardo UK.

References

[1] A. Sciarretta, G. D. Nunzio, and L. L. Ojeda, "Optimal Ecodriving Control," *IEEE Control Systems*, vol. 35, no. 5, pp. 71–90, 2015.

[2] I. Kolmanovsky and M. V. Nieuwstadt, "Optimization of Complex Powertrain Systems for Fuel Economy and Emissions," *Proceedings of the 1999 IEEE International Conference on Control Applications*, no. ii, 1999.

[3] L. Nielsen, M. Ivarsson, A. Jan, and E. Hellstro, "Look-ahead control for heavy trucks to minimize trip time and fuel consumption," *Control Engineering Practice*, vol. 17, pp. 245–254, 2009.

[4] R. Lot and S. A. Evangelou, "Green Driving Optimization of a Series Hybrid Electric Vehicle," in *52nd IEEE Conference on Decision and Control*, 2013, pp. 2200–2207.

[5] B. Saerens, A. Nv, and B. Saerens, "Optimal Control Based Eco- Driving Optimal Control Based Eco-Driving," Ph.D. dissertation, University of Leuven, 2012.

[6] W. Zhou, C. Zhang, J. Li, and H. K. Fathy, "A Pseudospectral Strategy for Optimal Power Management in Series Hybrid Electric Powertrains," *IEEE Transactions on Vehicular Technology*, vol. 65, no. 6, pp. 4813–4825, 2016.

[7] T. V. Keulen, B. D. Jager, and M. Steinbuch, "Optimal Trajectories for Vehicles with Energy Recovery Options ," in *IFAC Proceedings Volumes*, vol. 44, no. 1. IFAC, 2011, pp. 3831–3836. [Online]. Available: http://dx.doi.org/10.3182/20110828-6-IT-1002.02062

[8] F. Liu, W. W. Hager, and A. V. Rao, "An hp Mesh Refinement Method for Optimal Control Using Discontinuity Detection and Mesh Size Reduction," *53rd IEEE Conference on Decision and Control, Los Angeles*, pp. 5868–5873, 2014.

[9] T. Markel, A. Brooker, T. Hendricks, V. Johnson, K. Kelly, B. Kramer, M. O. Keefe, S. Sprik, and K. Wipke, "ADVISOR : a systems analysis tool for advanced vehicle modeling," *Journal of Power Sources*, vol. 110, pp. 255–266, 2002.

[10] G. Perantoni and D. J. N. Limebeer, "Optimal control for a Formula One car with variable parameters," *Vehicle System Dynamics*, vol. 3114, no. November, pp. 653–678, 2016. [Online]. Available: http://dx.doi.org/10.1080/00423114.2014.889315

[11] A. V. Rao, D. a. Benson, C. Darby, M. a. Patterson, C. Francolin, I. Sanders, and G. T. Huntington, "GPOPS II: A MATLAB Software for Solving Multiple-Phase Optimal Control Problems Using hpAdaptive Gaussian Quadrature Collocation Methods and Sparse Nonlinear Programming," *ACM Transactions on Mathematical Software*, vol. 37, no. 2, pp. 1–39, 2010. [Online]. Available: http://portal.acm.org/citation.cfm?doid=1731022.1731032

[12] M. J. Weinstein and A. V. Rao, "Algorithm : ADiGator , a Toolbox for the Algorithmic Differentiation of Mathematical Functions in MATLAB Using Source Transformation via Operator Overloading," *ACM Transactions on Mathematical Software*, vol. V, no. 212, pp. 1–32, 2015.

[13] W. Andreas, "On the implementation of an interior-point filter line-search algorithm for large-scale nonlinear programming," *Mathematical programming*, vol. 106, no. 1, pp. 25–57, 2006.